Immunity, Vol. 14, 523–534, May, 2001, Copyright ©2001 by Cell Press

T Cell-Specific Loss of Pten Leads to Defects in Central and Peripheral Tolerance

Akira Suzuki,[1,5,6] Manae Tsukio Yamaguchi,[1] Toshiaki Ohteki,[3] Takehiko Sasaki,[6] Tsuneyasu Kaisho,[2] Yuki Kimura,[6] Ritsuko Yoshida,[6] Andrew Wakeham,[6] Tetsuya Higuchi,[4] Manabu Fukumoto,[5] Takeshi Tsubata,[4] Pamela S. Ohashi,[7] Shigeo Koyasu,[3] Josef M. Penninger,[6] Toru Nakano,[1,8] and Tak W. Mak[6]

[1]Department of Molecular and Cellular Biology
[2]Department of Host Defense
Research Institute for Microbial Disease
Osaka University
Osaka 565-0871
[3]Department of Microbiology and Immunology
Keio University
Tokyo 160-8582
[4]Department of Immunology
Medical Research Institute
Tokyo Medical and Dental University
Tokyo 113-8510
[5]Department of Pathology
Institute of Development, Aging, and Cancer
Tohoku University
Miyagi 980-0801
Japan
[6]Amgen Institute
Ontario Cancer Institute and
University of Toronto
Toronto, Ontario M5G 2C1
[7]Ontario Cancer Institute and
Department of Medical Biophysics
University of Toronto
Toronto, Ontario M5G 2M9
Canada

Summary

***PTEN*, a tumor suppressor gene, is essential for embryogenesis. We used the Cre-loxP system to generate a T cell-specific deletion of the *Pten* gene (*Pten*$^{flox/-}$ mice). All *Pten*$^{flox/-}$ mice develop CD4$^+$ T cell lymphomas by 17 weeks. *Pten*$^{flox/-}$ mice show increased thymic cellularity due in part to a defect in thymic negative selection. *Pten*$^{flox/-}$ mice exhibit elevated levels of B cells and CD4$^+$ T cells in the periphery, spontaneous activation of CD4$^+$ T cells, autoantibody production, and hypergammaglobulinemia. *Pten*$^{flox/-}$ T cells hyperproliferate, are autoreactive, secrete increased levels of Th1/Th2 cytokines, resist apoptosis, and show increased phosphorylation of PKB/Akt and ERK. Peripheral tolerance to SEB is also impaired in *Pten*$^{flox/-}$ mice. PTEN is thus an important regulator of T cell homeostasis and self-tolerance.**

Introduction

Mutations of the tumor suppressor gene *PTEN* (also called *MMAC1* or *TEP1*) (Li et al., 1997) have been identified in many human sporadic cancers and in hereditary disorders such as Cowden disease and Bannayan-Riley-Ruvalcaba syndrome, which are characterized by multiple hamartomas and an increased risk of cancer (Liaw et al., 1997; Marsh et al., 1997). PTEN is a multifunctional phosphatase whose lipid phosphatase activity is associated with tumor suppression (Myers et al., 1998). The primary substrate of PTEN is thought to be phosphatidyl inositol-3,4,5-triphosphate (PIP3) (Maehama and Dixon, 1998), a molecule which mediates signaling promoting cell proliferation/survival and adhesion/migration (Toker and Cantley, 1997).

We and others previously generated *Pten*$^{-/-}$ null mutant knockout mice to examine the function of Pten in vivo (Suzuki et al., 1998; Di Cristofano et al., 1998; Podsypanina et al., 1999). However, *Pten*$^{-/-}$ mice die during early embryogenesis, precluding a functional analysis of Pten in various organs. We subsequently showed in *Pten*$^{-/-}$ embryonic fibroblasts that the survival kinase PKB/Akt is a key player downstream of Pten and that regulation of PKB/Akt activation by Pten is critical for normal apoptotic signaling induced by a variety of apoptotic stimuli (Stambolic et al., 1998). Mice heterozygous for the *Pten* null mutation often develop lymphoid hyperplasia, which progresses to T cell lymphoma in some cases (Suzuki et al., 1998; Podsypanina et al., 1999). In addition, *Pten*$^{+/-}$ mice have recently been reported to develop autoimmune disorders (Di Cristofano et al., 1999). These observations plus the finding of constitutive expression of *Pten* in T cells (Suzuki et al., 1998) implied that Pten might be crucial for normal T cell function and/or homeostasis.

Central T cell tolerance is established in the thymus by the clonal deletion of self-reactive thymocytes during negative selection (Kappler et al., 1987) and the positive selection of MHC-restricted CD8$^+$ and CD4$^+$ thymocytes (Teh et al., 1988; Kaye et al., 1989). Self-reactive T cells that escape into the periphery are controlled by mechanisms of peripheral tolerance, such as clonal deletion and functional inactivation (Webb et al., 1990). Despite intensive study (reviewed by Sebzda et al., 1999), the complex signaling pathways underlying the establishment of central and peripheral tolerance remain incompletely defined.

To investigate the role of Pten in T cell tolerance, we used the Cre-loxP conditional gene targeting system to generate mice in which Pten was disrupted in T cells. We describe the phenotype of *Lck-CrePten*$^{flox/-}$ mice and report results revealing possible mechanisms contributing to the autoimmunity and tumorigenesis observed in Pten-deficient mice.

Results

Generation of T Cell-Specific Pten-Deficient Mice

T cell-specific Pten-deficient mice (*Lck-CrePten*$^{flox/-}$; *Pten*$^{flox/-}$) were generated using the strategy described in Figure 1A and Experimental Procedures. *Pten*$^{flox/-}$ mice were born alive and appeared healthy. Genomic Southern blotting showed that, in the vast majority of thymo-

[8]Correspondence: tnakano@biken.osaka-u.ac.jp

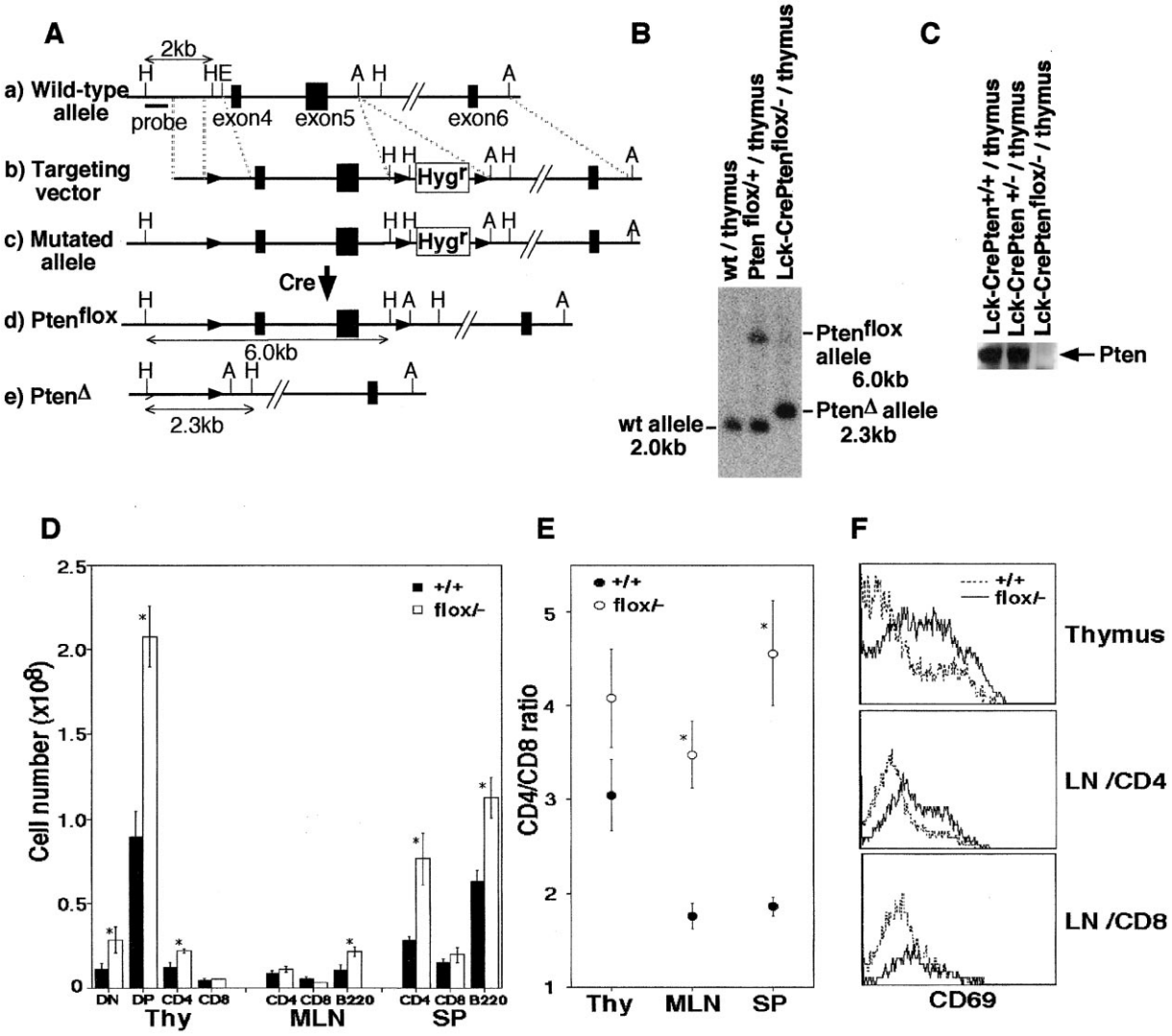

Figure 1. T Cell-Specific Gene Targeting and Altered Cell Populations in Lymphoid Organs of *Pten* $^{flox/-}$ Mice

(A) Construction of the targeting vector and mutant alleles. (Aa) Genomic structure of the mouse *Pten* gene. A, ApaI; E, EcoRI; H, HindIII. (Ab) The targeting vector. Exons 4 and 5 were flanked by two *loxP* sequences, shown as black arrowheads. A third *loxP* sequence was introduced to flank the *Hygr* gene. (Ac) The mutated allele containing three *loxP* sequences and the *Hygr* gene. Cre-mediated deletion was expected to produce the (Ad) *Ptenflox* allele and (Ae) *Pten*Δ allele.

(B) Southern blot analysis. DNA (20 μg) was extracted from thymocytes of mice of the indicated genotypes. Blots were hybridized to the probe indicated in Figure 1Aa. wt, wild-type.

(C) Western blot analysis of proteins from thymocytes of mice of the indicated genotypes.

(D) Absolute numbers of DN, DP, $CD4^+$, $CD8^+$, and $B220^+$ cells in the thymus (Thy), mesenteric lymph nodes (MLN), and spleen (SP).

(E) CD4/CD8 ratio in the thymus, MLN, and spleen.

(D and E) The results are expressed as the mean ± SEM for six mice of 6–8 weeks of age per group. +/+, *Lck-CrePten*$^{+/+}$ mice; flox/−, *Lck-CrePten*$^{flox/-}$ mice. Statistical differences were determined using the Student's t test; *, $p < 0.05$.

(F) CD69 expression in the thymus and in $CD4^+$ and $CD8^+$ populations of MLN (LN/$CD4^+$ and LN/$CD8^+$) of the mice analyzed in (D).

cytes, the *loxP* sites and the DNA between them in the 6.0 kb *Ptenflox* allele had been deleted, generating the 2.3 kb *Pten*Δ allele (Figure 1B). The deletion of *Pten* exons 4 and 5 was confirmed at the protein level by Western blotting using antibody recognizing the N terminus of Pten (Figure 1C).

Lymphadenopathy, Splenomegaly, and Enlarged Thymi in *Pten*$^{flox/-}$ Mice

Lck-CrePten$^{+/+}$ (*Pten*$^{+/+}$) and *Pten*$^{flox/-}$ mice were sacrificed at 6–8 weeks of age, and T cell subpopulations in the mesenteric lymph nodes (MLN), spleen, and thymus were examined. Total numbers of splenocytes, MLN cells, and thymocytes were increased in *Pten*$^{flox/-}$ mice 2.0-fold, 1.5-fold, and 2.2-fold, respectively (Figure 1D). No tumor formation was observed either macro- or microscopically at this stage. Flow cytometric analysis revealed that the total numbers of double-negative (DN; $CD4^-CD8^-$), double-positive (DP; $CD4^+CD8^+$), and $CD4^+$ single-positive (SP) cells were increased in the thymus from *Pten*$^{flox/-}$ mice. In the periphery, the total numbers of $CD4^+$ and $B220^+$ cells were increased, but

the number of $CD8^+$ cells was about normal (Figure 1D). A greater expansion or accumulation of $CD4^+$ T cells in the spleen than in the MLN led to a higher CD4/CD8 ratio in this organ (Figure 1E). Immunostaining to detect the T cell activation marker CD69 showed that *Pten*$^{flox/-}$ thymocytes and peripheral T cells were spontaneously activated, peripheral $CD4^+$ cells more so than $CD8^+$ cells (Figure 1F). Surface staining of B cells in bone marrow and spleen of *Pten*$^{flox/-}$ mice showed that the total numbers of pro-B, pre-B, and mature B cells were all increased proportionately (data not shown). No differences from the wild-type (wt) were observed in CD40 expression on B cells, or in CD40L, TCR$\alpha\beta$, CD28, or CD25 expression on T cells, in either splenic or MLN cell populations (data not shown).

Premature Death of *Pten*$^{flox/-}$ Mice Due to $CD4^+$ T Cell Lymphomas

To determine the impact on the whole animal of the T cell-specific Pten mutation, the health and development of 16 *Pten*$^{flox/-}$, 20 *Pten*$^{+/-}$, and 20 *Pten*$^{+/+}$ mice were monitored over a period of 1 year. Tumor formation was observed from 10 weeks of age (Figure 2A), and all 16 *Pten*$^{flox/-}$ mice died of malignant T cell lymphomas within 17 weeks (Figure 2B), exhibiting enlarged lymph nodes, spleen, thymus, and liver. Histologically, the lymphomas appeared as sheets of relatively homogeneous cells mixed with scattered tingible body macrophages to give a "starry-sky" appearance (Figure 2C). The lymphoma cells had scant cytoplasm, enlarged round nuclei, irregular nuclear contours, and prominent nucleoli (Figure 2D) compared to wt cells (Figure 2E). A massive invasion of lymphocytes occurred adjacent to the blood vessels in other tissues, such as liver (Figure 2F), kidney (Figure 2G), and lung (Figure 2H). *Pten*$^{+/-}$ mice, especially the females, began to show polyclonal lymphoid hyperplasia at 28 weeks, and 50% of these mice died within 1 year of birth. No *Pten*$^{+/+}$ mouse developed tumors during the 12 month observation period. About 90% of the T cell tumors in *Pten*$^{flox/-}$ mice could be classified as $CD4^+$ SP T cell lymphomas (Figure 2I), and 10% were a mixture of $CD4^+$ SP and DP lymphomas. $CD8^+$ SP T cell lymphomas were never observed. Monoclonality of invading lymphoma cells was detected in 12% of affected mice, using four antibodies reactive to specific TCR variable regions (Figure 2J).

Impaired Negative Thymic Selection in Pten-Deficient HY-TCR Transgenic Mice

To investigate the role of Pten in central tolerance, we crossed the *Lck-CrePten*$^{flox/-}$ mutation into HY-TCR transgenic (Tg) animals (C57BL/6J background; H-2^b; Kisielow et al., 1988) to generate *HYLck-CrePten*$^{flox/-}$ mice. The majority of thymocytes in HY-TCR Tg mice bear TCRs specific for the male antigen HY, such that they are positively selected in female mice but negatively selected in male mice of the H-2^b background. Positive and negative selection in the thymus were compared in *HYLck-CrePten*$^{+/+}$ and *HYLck-CrePten*$^{flox/-}$ mice. Consistent with published reports (Kisielow et al., 1988), negatively selecting male *HYLck-CrePten*$^{+/+}$ mice showed a marked reduction in total thymocyte numbers as well as a decrease in DP cells expressing the HY Tg TCR (Table 1 and Figure 3A). However, the total number of thymic DP cells as well as the number of thymic DP cells which expressed the Tg TCR was more than 10-fold greater in male *HYLck-CrePten*$^{flox/-}$ mice than in male *HYLck-CrePten*$^{+/+}$ mice, as detected by a clonotypic mAb specific for the Vβ8.2 chain (data not shown) or the T3.70 mAb specific for the transgenic Vα chain (Figure 3A and Table 1). These data indicate that HY-TCR *Pten*$^{flox/-}$ mice have a defect in thymic negative selection. It should be noted, however, that thymocyte numbers in *HYLck-CrePten*$^{flox/-}$ male mice were only reduced $\sim$2-fold compared to numbers in the thymi of positively selecting *HYLck-CrePten*$^{flox/-}$ female mice.

Histological comparison of tissues of 8- to 9-week-old male *HYLck-CrePten*$^{flox/-}$, *HYLck-CrePten*$^{+/+}$, and *Lck-CrePten*$^{flox/-}$ mice (not transgenic for the HY-TCR) showed a marked infiltration of small lymphoid cells into both perivascular areas and some alveolar septa of the lungs of all three male *HYLck-CrePten*$^{flox/-}$ mice examined (Figure 3B). Atypical cells were not detected, suggesting the occurrence of "lymphoid interstitial pneumonia," a disorder thought to be caused by autoimmune mechanisms (Staszak and Harbeck, 1985). No histological alterations were observed in four *HYLck-CrePten*$^{+/+}$ male or three *Lck-CrePten*$^{flox/-}$ male mice.

Positively selecting female *HYLck-CrePten*$^{+/+}$ mice showed a substantial increase in the $CD8^+$ SP population in the thymus compared to female *Lck-CrePten*$^{+/+}$ mice, consistent with the recognition of MHC class I by the HY-TCR transgene. An $\sim$2-fold decrease both in the number of transgenic $CD8^+$ SP cells (Figures 3C and 3D) and the CD8/CD4 ratio was observed in female *HYLck-CrePten*$^{flox/-}$ mice compared to female *HYLck-CrePten*$^{+/+}$ mice, while the number of transgenic $CD4^+$ SP cells was increased 1.5-fold. These results suggest that *HYLck-CrePten*$^{flox/-}$ mice are also impaired in the positive selection of $CD8^+$ cells in the thymus and that the DP precursor cells may be preferentially developing into $CD4^+$ cells. This is consistent with the increase in $CD4^+$ SP cells in the *HYLck-CrePten*$^{flox/-}$ male mice. Taken together, our data suggest that Pten influences both lineage commitment and negative thymic selection.

Superantigen-Induced Deletion of Peripheral T Cells

Peripheral tolerance was investigated using deletion of peripheral T cells induced by the superantigen staphylococcal enterotoxin B (SEB). SEB specifically recognizes TCRs containing Vβ8, such that V$\beta8^+$ peripheral T cells expand and are subsequently deleted in an animal injected with SEB (Kawabe and Ochi, 1991). As shown in Figure 3F, a single dose of SEB injected into the peritoneal cavity of a *Pten*$^{+/+}$ mouse induced an expansion of V$\beta8^+CD4^+$ T cells that peaked on day 2 postinjection, followed by deletion of this population by day 7. V$\beta8^+$ T cells from *Pten*$^{flox/-}$ mice expanded to almost the same degree as those from *Pten*$^{+/+}$ mice but were resistant to deletion and had not declined below preinjection levels even by day 14 (Figure 3E). Control V$\beta6^+CD4^+$ peripheral T cells, whose TCRs are not recognized by SEB, failed to undergo deletion (Figure 3F). SEB-induced peripheral deletion is thus impaired in the absence of Pten, suggesting that Pten is involved in the establishment of peripheral tolerance.

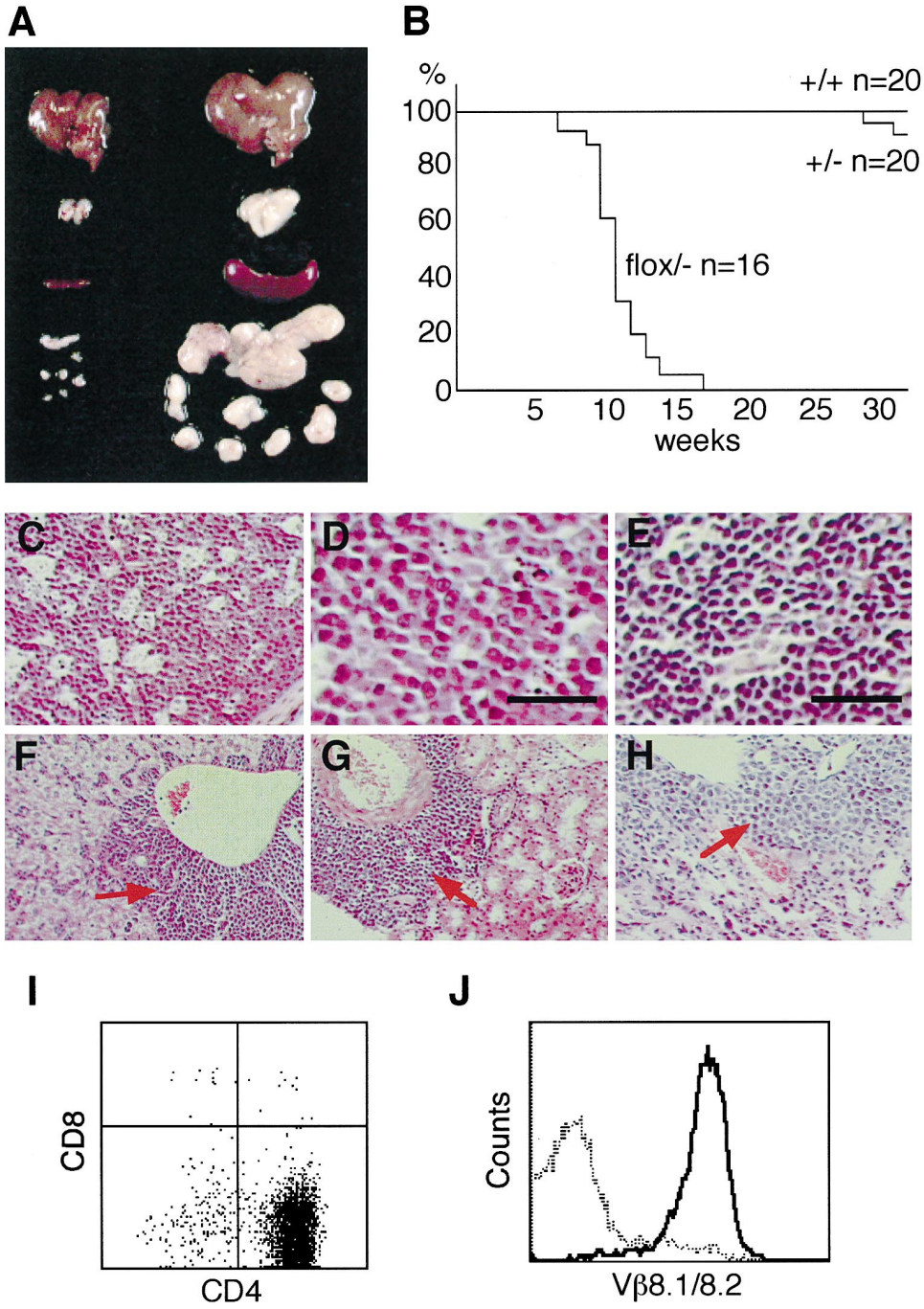

Figure 2. Spontaneous Development of CD4$^+$ T Cell Lymphomas

(A) *Pten*$^{flox/-}$ mice develop lymphomas with massive hepatolymphoid organomegaly (right panel). Left panel shows the same organs in a control *Pten*$^{+/+}$ mouse.

(B) Survival curve of *Pten*$^{flox/-}$ mice compared to wild-type (+/+) and heterozygous (+/−) mice.

(C–H) Histology. Mesenteric lymph node of a lymphoma-bearing *Pten*$^{flox/-}$ mouse (C), lymphoma cells in the spleen of a *Pten*$^{flox/-}$ mouse (D), and the spleen of a wild-type mouse (E); bar represents 30 μm. Infiltrate (red arrow) in liver (F), kidney (G), and lung (H) of a *Pten*$^{flox/-}$ mouse.

(I) Flow cytometric profile of CD4/CD8 staining of the enlarged lymph node of an *Lck-CrePten*$^{flox/-}$ mouse.

(J) TCR Vβ8 staining of CD4$^+$ cells from the enlarged lymph node analyzed in (I). MLN CD4$^+$ cells from a *Pten*$^{+/+}$ mouse were used as a control.

Autoreactivity of Pten-Deficient T Cells

To determine whether T cells in *Pten*$^{flox/-}$ mice were autoreactive, mixed lymphocyte reactions (MLR) were performed. Irradiated splenocytes (stimulators) from syngeneic C57BL6/J mice (Figure 4A, left) or allogeneic DBA1 mice (Figure 4A, right) were cocultured with *Pten*$^{+/+}$ or *Pten*$^{flox/-}$ T cells (responders) from 6- to 8-week-old mice, and proliferation was assayed by [^{3}H]thymidine uptake.

Table 1. Profile of HY-TCR Transgenic Model

	Male							Female	
	$Tg^{-}Pten^{+/+}$	$Tg^{+}Pten^{+/+}$	$Tg^{+}Pten^{+/+}$	$Tg^{+}Pten^{+/+}$	$Tg^{+}Pten^{flox/-}$	$Tg^{+}Pten^{flox/-}$	$Tg^{+}Pten^{flox/-}$	$Tg^{+}Pten^{+/+}$	$Tg^{+}Pten^{flox/-}$
Thymus ($\times 10^6$)	135	16	17	21	110	75	53	140	190
$CD4^{+}CD8^{+}$ (%)	76	9.3	4.9	11	35	61	32	58	66
$CD4^{+}CD8^{+}$ ($\times 10^6$)	100	1.5	0.81	2.2	38	46	17	84	130
T3.70 (%)	—	67	49	51	58	48	40	26	21
T3.70 ($\times 10^6$)	—	11	8.0	11	64	36	21	36	40
Spleen ($\times 10^6$)	110	120	150	100	210	450	345	—	—
T3.70 ($\times 10^6$)	—	50	53	25	95	142	94	—	—

Total thymocytes and spleen cells were isolated from the *HYLck-CrePten*$^{+/+}$ and *HYLck-CrePten*$^{flox/-}$ mice in negative-selecting (male, H-2^b) and positive-selecting backgrounds (female, H-2^b) and control *Pten*$^{+/+}$ mice. All mice were aged matched. Cells were stained simultaneously with anti-CD8 (FITC), anti-CD4 (PE), and T3.70 antibody (biotin), which recognizes the transgenic TCR Vα chain. T3.70 antibody was visualized using streptoavidin-Red 670. Samples were analyzed using a FACSCalibur.

Interestingly, the already enhanced proliferative capacity of *Pten*$^{flox/-}$ T cells was further increased when the cells were cocultured not only with the allogeneic stimulators but also the syngeneic stimulators, indicating that *Pten*$^{flox/-}$ T cells are autoreactive.

To investigate whether the loss of Pten in T cells also affected self-tolerance in the humoral response, serum Ig levels and autoantibody titers were assessed in *Pten*$^{flox/-}$ mice of 6–8 weeks of age. Levels of IgG1, IgG2b, IgM, and IgA were elevated in *Pten*$^{+/-}$ mice compared to *Pten*$^{+/+}$ mice (Figure 4B), and the level of IgG1 was increased still further in *Pten*$^{flox/-}$ mice. Serum anti-ssDNA Ab were measured at 6–8 weeks (Figure 4C, left) and 6–8 months (Figure 4C, right). *Pten*$^{+/-}$ mice of 6–8 months of age, especially those exhibiting lymphoid hyperplasia, produced significantly greater amounts of anti-ssDNA Ab compared to *Pten*$^{+/+}$ mice. *Pten*$^{flox/-}$ mice died before 6 months of age, but titers of anti-ssDNA Ab in 6- to 8-week-old *Pten*$^{flox/-}$ mice were higher than those of *Pten*$^{+/+}$ or *Pten*$^{+/-}$ mice of the same age. Interestingly, this titer was still lower than that of 6- to 8-month-old *Pten*$^{+/-}$ mice with lymphoid hyperplasia. Taken together, our data suggest that Pten is required for normal self-tolerance in both the humoral and cell-mediated branches of the immune response.

Enhanced Proliferation and Cytokine Production of *Pten*$^{flox/-}$ T Cells

To examine the function of peripheral T cells in *Pten*$^{flox/-}$ mice, purified MLN T cells were stimulated in vitro with the stimuli indicated in Figure 5A. Whereas *Pten*$^{+/+}$ and *Pten*$^{flox/-}$ T cells proliferated equally well in response to PMA plus Ca^{2+}-ionophore, *Pten*$^{flox/-}$ T cells showed enhanced proliferation in response to anti-CD3ϵ, ConA, or IL-2 stimulation. Addition of anti-CD28 or IL-2 to anti-CD3ϵ synergistically increased the proliferation of *Pten*$^{+/+}$, *Pten*$^{+/-}$, and *Pten*$^{flox/-}$ T cells. Cytokine production by purified MLN T cells stimulated with anti-CD3ϵ plus anti-CD28 mAbs or ConA was measured using ELISA. Activated *Pten*$^{flox/-}$ T cells produced significantly higher levels of both Th1 (IL-2 and IFNγ) and Th2 (IL-4, IL-6, and IL-10) cytokines compared to *Pten*$^{+/-}$ or *Pten*$^{+/+}$ cells (Figure 5B). This increase in IL-10 and IL-4, cytokines that favor immunoglobulin class switching to IgG1 (Briere et al., 1994; Esser and Radbruch, 1989), may at least partially account for the enhanced level of serum IgG1 and the increased B cell number observed in *Pten*$^{flox/-}$ mice. Our data show that loss of Pten in T cells results in increased proliferation and enhanced cytokine production of Th1 and Th2 cytokines.

Decreased Apoptosis of *Pten*$^{flox/-}$ Thymocytes and Peripheral T Cells In Vitro

To determine whether the loss of self-tolerance in Pten-deficient mice could be partially due to a defect in thymocyte apoptosis, we evaluated the responses of *Pten*$^{flox/-}$ thymocytes to treatment in vitro with various apoptotic stimuli as described in Figure 5C. Loss of Pten conferred resistance to apoptosis, particularly to cell death induced by the specific adenosine receptor agonists N6-[4-[[[4-[[[(2-aminoethyl)amino]carbonyl]methyl]-anilino] carbonyl]methyl]phenyl]adenosine (ADAC, RBI; Figure 5CH) and 2-p-(2-carboxyethyl)phenethylamino-59-N-ethylcar-boxamidoadenosine hydrochloride (CGS-21680, Sigma; Figure 5CI) (Sasaki et al., 2000). A more modest but still significant antiapoptotic effect was obtained when *Pten*$^{flox/-}$ thymocytes were stimulated with γ irradiation or UV (Figures 5CF and 5CG, respectively). No statistically significant differences in apoptosis were observed following treatment with anti-CD3ϵ, dexamethasone, adriamycin, anti-Fas antibody, or serum withdrawal (Figures 5CA, 5CB, 5CC, 5CD, and 5CE, respectively).

To determine whether Pten influences peripheral T cell survival, peripheral T cells were treated in vitro with a variety of apoptotic stimuli as described in Figure 5D (left). A moderate antiapoptotic effect was obtained when *Pten*$^{flox/-}$ T cells were stimulated with anti-Fas Ab (Figure 5DA), γ irradiation (Figures 5DB and 5DC), or UV (low levels; Figure 5DD). No significant differences between *Pten*$^{flox/-}$ and *Pten*$^{+/+}$ cells were observed in apoptotic responses to anti-CD3ϵ mAb or adriamycin (Figures 5DF and 5DG, respectively). However, dramatic resistance to apoptosis was observed in *Pten*$^{flox/-}$ T cells from which IL-2 or IL-2 plus serum were withdrawn (Figures 5DH and 5DI, respectively). By 48 hr after withdrawal of IL-2, only 46% of *Pten*$^{+/+}$ T cells remained viable, compared to 98% of *Pten*$^{flox/-}$ cells (Figure 5D, right). These results indicate that loss of Pten prevents T cells from initiating apoptosis in response to several stimuli, including some known to be mutagenic.

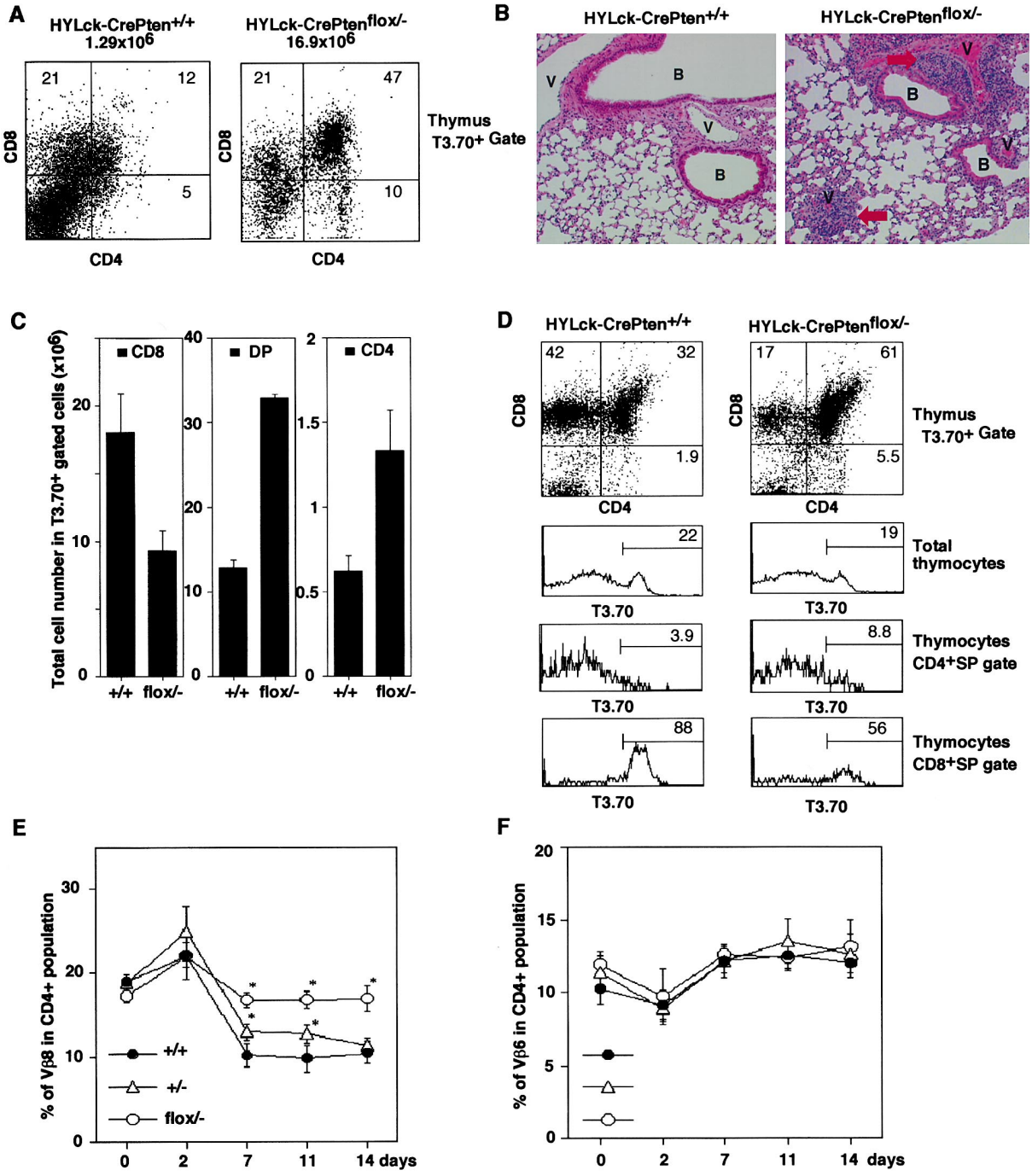

Figure 3. Altered Central and Peripheral Tolerance in *Pten*$^{flox/-}$ Mice

(A and B) Impaired thymic negative selection in Pten-deficient HY-TCR transgenic mice.

(A) Thymocytes from 8-week-old *Lck-CrePten*$^{flox/-}$ (n = 8) and *Lck-CrePten*$^{+/+}$ (n = 6) HY-TCR Tg mice in a negatively selecting background (H-2^b, male) were triple stained with anti-CD4-FITC, anti-CD8-PE, and T3.70-biotin mAb, and flow cytometric analysis was performed. Representative CD4 and CD8 profiles gated on T3.70$^+$ thymocytes. Numbers within the panels indicate the relative percentages of positively stained cells in the gated sample. Total numbers of T3.70$^+$CD4$^+$CD8$^+$ thymocytes for one representative experiment are shown.

(B) Lymphoid interstitial pneumonia in the lung of a male *HYLckCrePten*$^{flox/-}$ mouse (right). Lung from a male *HYLck-CrePten*$^{+/+}$ mouse as a control (left). Small lymphocytes (arrow) have infiltrated into the perivascular areas and some alveolar septa. B, bronchus; V, blood vessels.

(C and D) Altered thymic positive selection in Pten-deficient HY-TCR transgenic mice. Thymocytes from 8-week-old *Lck-CrePten*$^{flox/-}$ (n = 5) and *Lck-CrePten*$^{+/+}$ (n = 8) HY-TCR Tg mice in a positively selecting background (H-2^b, female) were triple stained with anti-CD4-FITC, anti-CD8-PE, and T3.70-biotin mAb.

(C) Total numbers of CD8$^+$, DP, and CD4$^+$ cells in T3.70$^+$ thymocytes.

(D) Representative CD4 and CD8 profiles gated on T3.70$^+$ thymocytes (upper panel); proportion of T3.70$^+$ cells in total thymocytes (second panel), in CD4$^+$ SP thymocytes (third panel), and in CD8$^+$ SP thymocytes (lower panel). Numbers within panels indicate the relative percentages of positively stained cells in the gated sample.

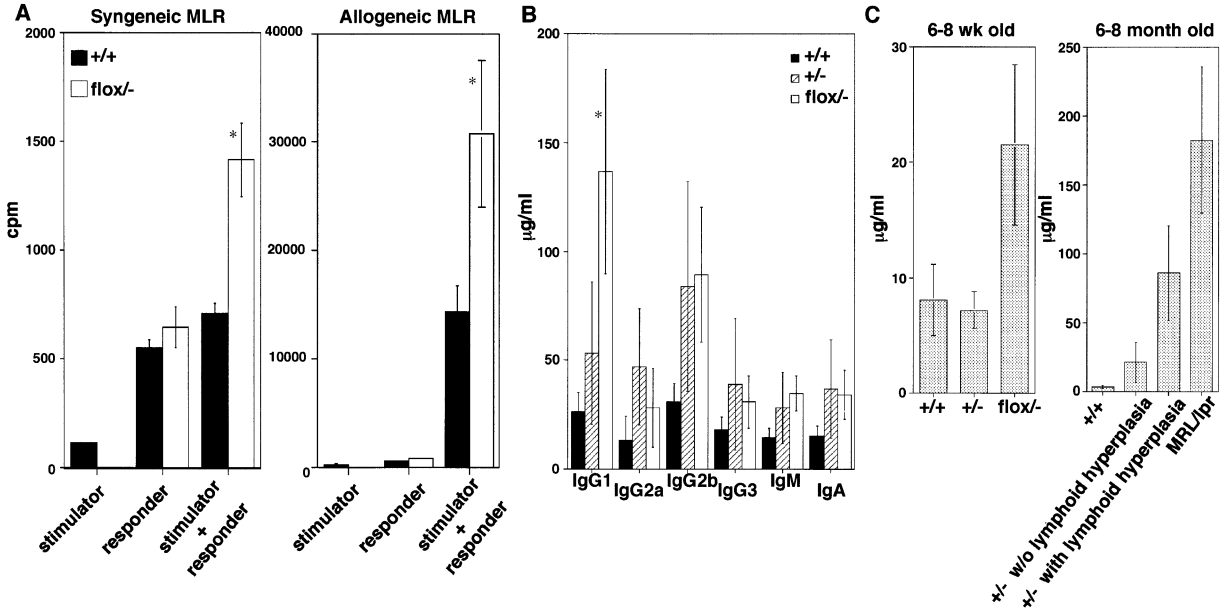

Figure 4. Autoreactivity of Pten-Deficient T Cells

(A) MLR. Responder T cells from *Pten*$^{flox/-}$ or *Pten*$^{+/+}$ mice were incubated with stimulator T cells from syngeneic C57BL/6J (left) or allogeneic DBA1 (right) mice. Proliferation was measured as mean thymidine uptake (cpm) ± SEM for three mice per group. Statistical differences were determined using the Student's t test; *, $p < 0.05$.

(B) Concentration of mean serum Ig levels in 6- to 8-week-old *Pten*$^{+/+}$ (n = 8), *Pten*$^{+/-}$ (n = 6), and *Pten*$^{flox/-}$ (n = 8) mice as determined by ELISA. Statistical differences were measured using the Welch's test. *, $p < 0.05$.

(C) Concentration of serum anti-ssDNA autoantibodies in 6- to 8-week-old mice (left panel) and 6- to 8-month-old mice (right panel) as determined by ELISA. Left panel (from left to right): *Pten*$^{+/+}$ (n = 3), *Pten*$^{+/-}$ (n = 3), and *Pten*$^{flox/-}$ (n = 3) mice. Right panel (from left to right): *Pten*$^{+/+}$ (n = 3), *Pten*$^{+/-}$ mice without lymphoid hyperplasia (n = 6), *Pten*$^{+/-}$ mice with lymphoid hyperplasia (n = 6), and positive control MRL/lpr mice (n = 3) of 4–6 months of age. Results are shown as the mean ± SEM.

Expression of Molecules Downstream of Pten in *Pten*$^{flox/-}$ T Cells

To identify molecules that might be responsible for the phenotypes of the *Pten*$^{flox/-}$ mice, the expression of various candidate proteins potentially acting downstream of Pten was analyzed by immunoblotting. We have previously reported that regulation of PKB/Akt activation by Pten is critical for normal apoptosis in embryonic fibroblasts (Stambolic et al., 1998) and possibly for oncogenesis. We therefore analyzed the phosphorylation of PKB/Akt in *Pten*$^{flox/-}$ peripheral T cells. Following stimulation with anti-CD3ε and anti-CD28 mAbs and/or IL-2, the phosphorylation of PKB/Akt was reproducibly elevated in *Pten*$^{flox/-}$ peripheral T cells compared to *Pten*$^{+/+}$ cells (Figure 6A). Importantly, the increase in PKB/Akt phosphorylation was paralleled by an increase in PKB/Akt kinase activity in *Pten*$^{flox/-}$ T cells relative to controls (Figure 6B). Increases in ERK phosphorylation (Gu et al., 1998) and Bcl-X_L expression (Jones et al., 2000) were also consistently observed, although no reproducible differences were found in the expression levels of candidate signaling molecules such as IκBα (Romashkova and Makarov, 1999; Ozes et al., 1999; Jones et al., 2000), Bcl-2 (Pugazhenthi et al., 2000), c-myc (Ghosh et al., 1999), phospho-p38 (Sugawara et al., 1998), $p27^{KIP}$ (Li and Sun, 1998), or phospho-BAD (Datta et al., 1997; del Peso et al., 1997) (Figure 6C and data not shown). Our results suggest that at least some of the phenotypes of *Lck-CrePten*$^{flox/-}$ mice maybe caused by disregulated PKB/Akt and ERK activation.

Discussion

In this study, we have described a novel system for evaluating the role of the multifunctional phosphatase Pten in murine T cell development and function. The Cre-loxP system was used to generate a T cell-specific mutation of Pten in mice, and defects of central and peripheral T cell tolerance were identified. Our data are highly relevant in the context of investigating whether PTEN links autoimmunity and tumorigenesis.

Roles for Pten in Thymic and Peripheral Tolerance

We have demonstrated, using the HY-TCR transgenic system, that there is a modest but definite defect in thymic negative selection in *Pten*$^{flox/-}$ mice. However, repeated experiments failed to reveal a difference in anti-CD3 mAb-induced apoptosis of *Pten*$^{+/+}$ and

(E and F) Impaired peripheral tolerance following SEB injection in vivo. *Pten*$^{+/+}$ (n = 12), *Pten*$^{+/-}$ (n = 8), and *Pten*$^{flox/-}$ (n = 7) mice were injected i.p. with SEB on day 0. Peripheral blood cells were stained with anti-Vβ8.1/8.2-FITC and anti-CD4-PE (E) or with anti-Vβ6-FITC and anti-CD4-PE (F) and analyzed by flow cytometry as indicated. Results are expressed as the mean ± SEM. Statistical differences were determined using the Welch's test; *, $p < 0.05$.

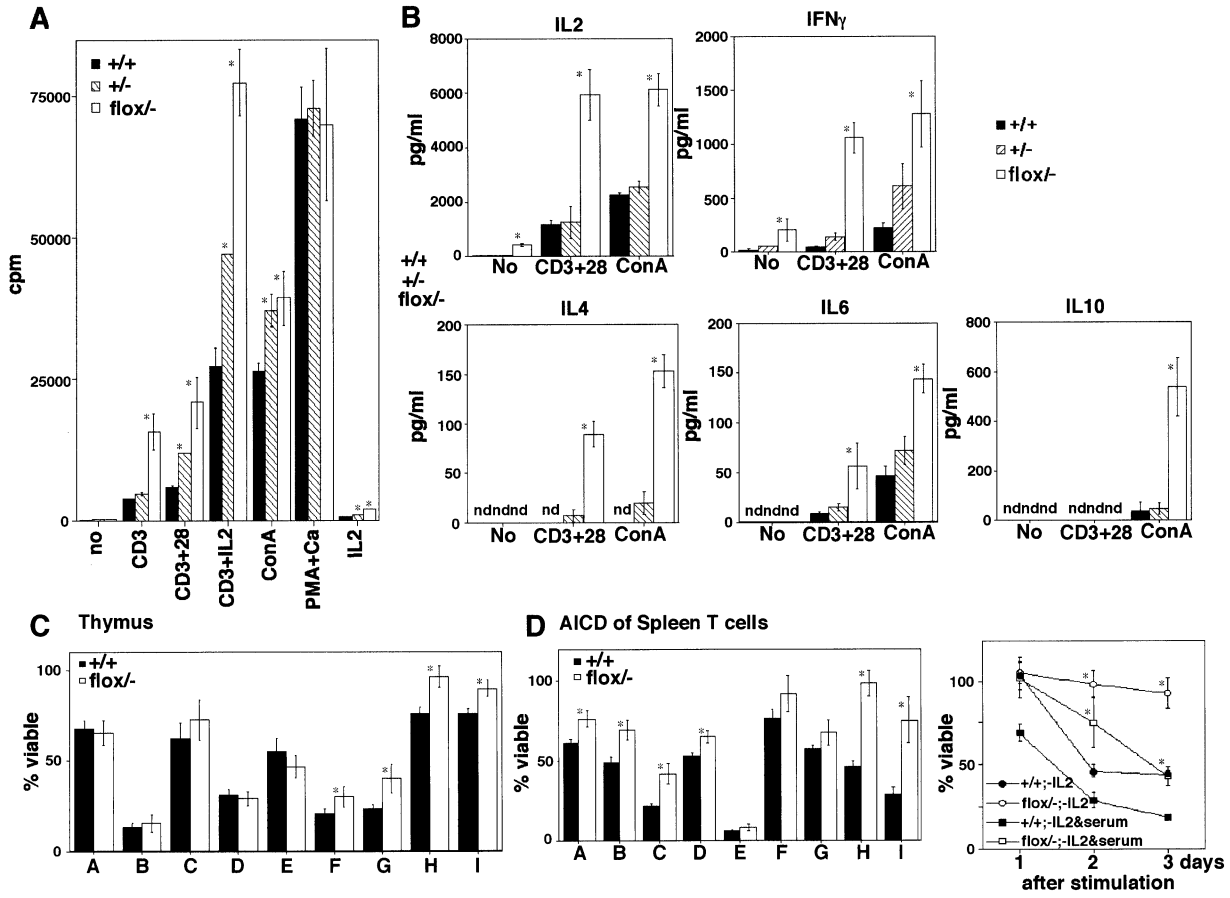

Figure 5. Increased Proliferation and cytokine Production but Defective Induction of Apoptosis in Pten-Deficient Thymocytes and Peripheral T Cells

(A–D) Statistical differences were determined using the Student's t test; *, $p < 0.05$.

(A) Enhanced proliferation of MLN T cells. Purified MLN T cells from 6-week-old *Pten*$^{+/+}$, *Pten*$^{+/-}$, and *Pten*$^{flox/-}$ mice were incubated with the indicated stimuli, and proliferation was measured by thymidine uptake. Mean thymidine uptake ± SEM for three mice per group is shown.

(B) Enhanced cytokine production by Pten-deficient T cells. Supernatants of cultures of purified splenic T cells stimulated with anti-CD3ε plus anti-CD28 mAbs or ConA for 30 hr were assayed by ELISA for the production of IL-2, IFNγ, IL-4, IL-6, and IL-10 as indicated. Results shown are the mean ± SEM for three mice per group. No, no stimulus; nd, not detected.

(C) Thymocyte apoptosis. Thymocytes from 6-week-old mice were stimulated for 24 hr with immobilized anti-CD3ε (10 μg/ml [CA]), dexamethazone (0.01 M [CB]), adriamycin (0.2 μg/ml [CC]), anti-Fas (1 μg/ml [CD]), γ irradiation (1 Gy [CF]), UV irradiation (3 J/m^2 [CG]), or for 48 hr with serum withdrawal (CE) or the adenosine receptor agonists ADAC (10 μM [CH]) or CGS-21680 (10 μM [CI]). Cell viability was determined by 7-AAD or Annexin V-PI staining followed by flow cytometry. The percentage of viable cells remaining after treatment as compared with the viability of untreated cells cultured for the same length of time is shown. Results are expressed as the mean ± SEM for nine mice per group.

(D) AICD of peripheral T cells. (Left panel) Splenic T cells were activated for 48 hr with anti-CD3ε and rIL-2 prior to treatment with apoptotic stimuli as follows: anti-Fas (1 μg/ml [DA]), γ irradiation (3 Gy [DB] and 10 Gy [DC]), UV irradiation (5 J/m^2 [DD] and 30 J/m^2 [DE]), anti-CD3ε (10 μg/ml [DF]), adriamycin (0.2 μg/ml [DG]), withdrawal of IL-2 alone (DH), or withdrawal of both IL-2 and serum (DI). Cell viability was determined as in Figure 5C. (Right panel) Time course of cell viability after cells were subjected to withdrawal of IL-2 and/or serum as indicated. The results are expressed as the percentage of viable cells remaining compared to untreated cells cultured with IL-2 for the same length of time.

Pten$^{flox/-}$ T cells. Alteration in thymic negative selection may thus involve a survival pathway other than that triggered by TCR signaling. Alternatively, stimulation by anti-CD3 in vitro may not fully replicate TCR engagement in vivo.

HY-TCR Tg *Pten*$^{flox/-}$ mice also showed impaired maturation of CD8$^+$ cells, which may explain why the numbers of CD8$^+$ T cells do not increase in the absence of Pten, even though Pten deficiency results in the expansion of all other T cell subpopulations in the thymus and peripheral lymphoid organs. A defect in lineage commitment rather than positive selection could lead to an increase in CD4$^+$ cells at the expense of CD8$^+$ cells. For example, a reduction in Notch 1 expression can induce CD8$^+$ cells to differentiate into CD4$^+$ cells (Yamamoto et al., 2000). However, no differences in Notch 1 expression were observed in *Pten*$^{+/+}$ and *Pten*$^{flox/-}$ thymocytes and peripheral T cells (data not shown). Similarly, mice deficient for the T cell activation molecule Itk have normal numbers of T cells but display a marked reduction in the CD4$^+$ subset (Liao and Littman, 1995). Itk-deficient T cells also show decreased proliferation in response to TCR engagement. Pten deficiency has been shown to result in constitutive tyrosine phosphory-

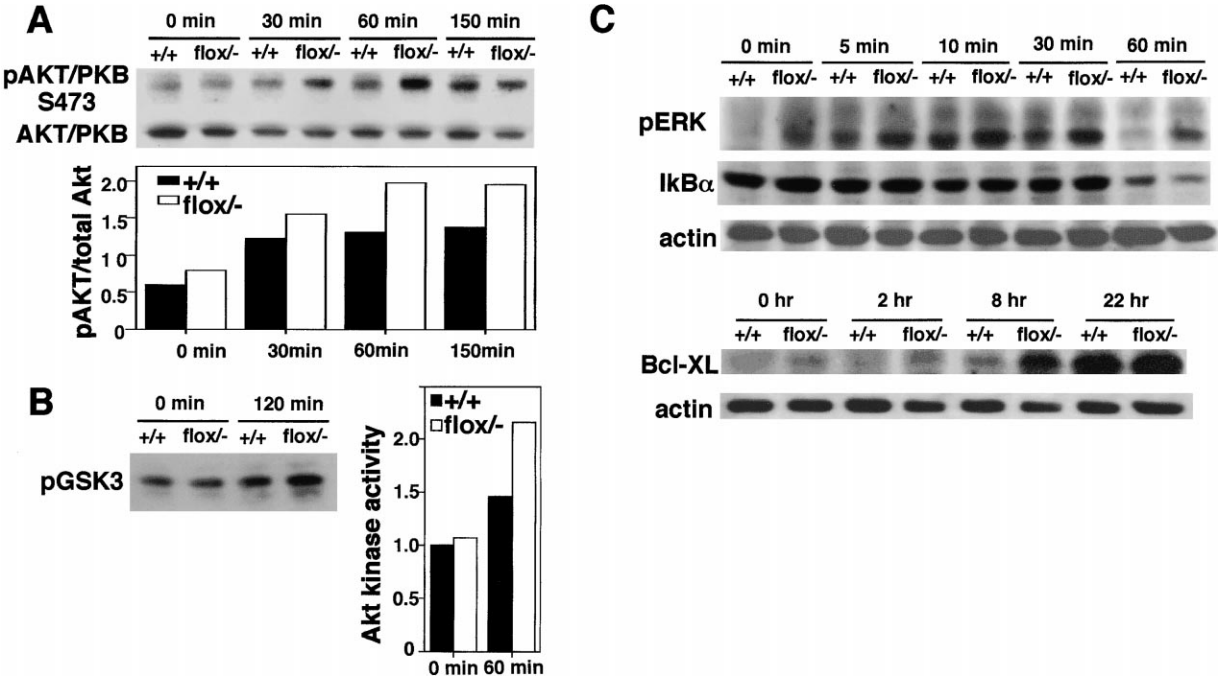

Figure 6. Increased Phosphorylation of PKB/Akt and ERK in *Pten*$^{flox/-}$ T Cells in Response to TCR Stimulation

Whole-cell lysates were extracted from purified *Pten*$^{+/+}$ and *Pten*$^{flox/-}$ peripheral T cells from 6-week-old mice. Cells were stimulated with immobilized anti-CD3ε and anti-CD28 (A and B) or anti-CD3ε and anti-CD28 plus IL-2 (C) for the indicated times. (A) (Upper panel) Western blot of the expression of phospho-PKB/Akt and PKB/Akt (control) in 20 μg extract protein. (Lower panel) Densitometric quantitation of phospho-PKB/Akt levels relative to total cellular PKB/Akt. (B) (Left panel) PKB/Akt kinase activity using pGSK-3 fusion protein as substrate. (Right panel) Densitometric quantitation of phosphoGSK-3 levels relative to controls. (C) Western blots of expression of pERK, IκBα, Bcl-X_L, and actin in 30 μg extract protein. The data are representative of three to seven independent experiments.

lation of Itk and permanent localization of this molecule in the plasma membrane (Shan et al., 2000). A prominent signaling molecule downstream of Itk is ERK, known to influence CD4/CD8 commitment. Development of CD4$^+$ cells is increased when ERK activity is increased, while that of CD8$^+$ cells is increased when ERK is decreased (Sharp and Hedrick, 1999). It is possible that the deficiency of Pten in T cells of our mutant mice leads to increased ERK signaling, biasing T cell differentiation toward CD4$^+$ and away from CD8$^+$. Such a scenario might account for the accumulation of CD4$^+$ cells in *Pten*$^{flox/-}$ mice.

In vivo SEB injection revealed that peripheral tolerance was also impaired in *Pten*$^{flox/-}$ mice. Fas signaling is reportedly involved in SEB-induced tolerance (Kim et al., 1991), and a defect in Fas signaling has been proposed as the basis of autoimmunity in *Pten*$^{+/-}$ mice (Di Cristofano et al., 1999). However, in our hands, while Vβ8$^+$CD4$^+$ cells from C57BL/6-*lpr/lpr* mice resist deletion compared to Vβ8$^+$CD4$^+$ cells from C57BL/6 mice, a marked reduction in cell numbers compared to the preinjection level is still observed (data not shown). In contrast, numbers of Vβ8$^+$CD4$^+$ cells from *Pten*$^{flox/-}$ mice were never significantly reduced compared to the preinjection level. These data suggest that the impairment in peripheral tolerance in *Pten*$^{flox/-}$ mice may be due to more than just a defect in Fas signaling. Experiments to compare SEB-induced deletion in *Pten*$^{flox/-}$ and *lpr/lpr* mice of identical genetic background and in *Pten/lpr* double mutant mice are in progress.

Molecules Contributing to the Phenotype of *Pten*$^{flox/-}$ T Cells

PTEN influences intracellular signaling via the PIP3 pathway. We have recently generated mice deficient for another key component of the PIP3 pathway, the p110γ catalytic subunit of phosphoinositide-3-kinase γ (PI3Kγ) (Sasaki et al., 2000). Several lines of evidence suggest that p110γ deficiency and Pten deficiency have opposite effects. Unlike *Pten*$^{-/-}$ mice, p110γ-deficient mice are viable, exhibiting decreased numbers of splenic CD4$^+$ SP cells. Proliferation of *p110*γ$^{-/-}$ T cells is reduced in response to all stimuli tested (except PMA + Ca ionophore), and *p110*γ$^{-/-}$ thymocytes are more susceptible to apoptotic stimuli, such as ADAC and CGS. Interestingly, deficiency for the PI3K regulatory subunit p85α leads to a partial block in early B cell development, but T cell development is not impaired (Suzuki et al., 1999; Fruman et al., 1999). A *p65*^{PI3K} transgenic mouse was recently described (Borlado et al., 2000) that expresses a constitutively active truncated form of p85α in T cells and exhibits phenotypes very similar to those of *Pten*$^{flox/-}$ mice. Lymphoproliferation and autoimmune disease characterized by an increased number of T cells, particularly CD4$^+$ cells, were observed in *p65*^{PI3K} Tg mice. Furthermore, these animals develop early T cell lymphomas when crossed into a *p53*$^{-/-}$ background. A comparison of the phenotypes of *p110*γ$^{-/-}$, *p65*^{PI3K} Tg, and *Pten*$^{flox/-}$ mice suggests that the abnormalities in *Pten*$^{flox/-}$ mice are likely due to hyperactivation of the PIP3 pathway.

Numerous studies have demonstrated inappropriate

activation of PKB/Akt in Pten-deficient tumor cells (Suzuki et al., 1998; Haas-Kogan et al., 1998), pointing to an important role for PKB/Akt in oncogenesis. While activation of PKB/Akt and Bcl-X_L was increased in stimulated *Pten*$^{flox/-}$ T cells compared to controls, levels of the downstream molecule IκBα were not altered. It may be that the modest activation of PKB/Akt induced in the absence of Pten in T cells is insufficient to induce the degradation of IκBα. Transgenic mice in which PKB/Akt is constitutively activated in T cells develop lymphoma and autoimmune disease characterized by a defect in Fas-mediated apoptosis (M.J. Parsons, personal communication). Interestingly, thymic selection is not impaired in these animals (Jones et al., 2000), suggesting that the onset of autoimmune disease in *Pten*$^{flox/-}$ mice may not necessarily be related to their defect in thymic negative selection. Indeed, most of the other phenotypes in the T cell-specific Pten-deficient mice can be explained by inappropriate activation of the PI3K/MAPK and PI3K/PKB/Akt pathways. It may be that the dramatic oncogenesis observed in Pten-deficient animals is due to perturbations of signaling pathways other than the PI3K pathway that accelerate the onset of lymphoma.

Role for PTEN in Linking Autoimmunity and Cancer?

In humans, germinal mutations in the *PTEN* gene cause Bannayan-Riley-Ruvalcaba syndrome, an oncogenic disorder frequently accompanied by Hashimoto thyroiditis, an autoimmune disease (Marsh et al., 1999). A common characteristic in syndromes arising from PTEN germline mutations is hamartomatous disease, in which abnormal stromal elements, such as mesenchymal or inflammatory cells, influence surrounding cells to become malignant. This phenomenon, termed the "landscaper's effect," has been observed in disorders such as juvenile polyposis syndrome (Kinzler and Vogelstein, 1998). It is possible that Pten deficiency promotes the accumulation of T cells that can mediate a landscaper's effect leading to malignancy.

While numerous studies have shown that a history of autoimmune disease increases the risk of cancer (Volkers, 1999), the molecules linking autoimmune disease to cancer are unknown. We have shown here that Pten-deficient mice, which develop T cell lymphomas, exhibit defects in central and peripheral tolerance. We continue to explore the role of impaired central tolerance in the manifestation of autoimmunity in these animals. Further experimentation may well show that PTEN is a key link between autoimmunity and tumorigenesis.

Experimental Procedures

Construction of the Targeting Vector

The conditional targeting vector (shown in Figure 1A) was constructed to delete a genomic fragment containing exons 4 and 5 of the *Pten* gene by homologous recombination. Exon 5 encodes the phosphatase domain essential for Pten-mediated dephosphorylation of PIP3 and tumor suppressor function. One *loxP* site was introduced into intron 3 and two into intron 5, such that *Pten* exons 4 and 5 were flanked by the intron 3 and one intron 5 *loxP* sites. The hygromycin resistance gene (*Hyg*^{r}) fused to the phosphoglycerokinase (*PGK*) promotor (*pGK-HYG*^{r}) was inserted in antisense orientation between the two *loxP* sites in intron 5. The 960 bp genomic fragment 5′ upstream of exon 4 and the 11.9 kb ApaI-ApaI fragment 3′ of exon 5 were inserted as the short and long arms, respectively. Not only was Cre-mediated deletion of exons 4 and 5 expected to inactivate Pten function, but the deletion also caused a frame shift, completely disrupting the rest of the protein coding sequence.

Generation of *Lck-CrePten*$^{flox/-}$ and HY-TCR Tg *Lck-CrePten*$^{flox/-}$ Mice

The linearized targeting vector was electroporated into E14K embryonic stem (ES) cells (H-2^b haplotype). Selection of targeted clones was carried out in 150 μg/ml hygromycin. Hygromycin-resistant clones were screened for homologous recombination by PCR following identification by genomic Southern blot as shown in Figure 1B. Correctly targeted clones were transiently transfected with *pMC1-Cre* (Gu et al., 1993) to delete the *loxP*-flanked *pGK-Hyg*^{r} gene. Progeny clones that became sensitive to hygromycin were subjected to Southern blot analysis to detect those retaining exons 4 and 5 flanked by two *loxP* sites (the *Ptenflox* allele) and those lacking exons 4 and 5 (*Pten*Δ allele; equivalent to a knockout mutation). Five *Pten*$^{flox/+}$ ES clones were microinjected into C57BL/6 blastocysts to generate chimeric mice. Three chimeric mice successfully transmitted the mutation to the germline.

To generate T cell-specific Pten-deficient mice, chimeric mice were backcrossed three times to C57BL6/J mice to give *Pten*$^{flox/+}$ mice. *Pten*$^{flox/+}$ mice were mated to *Lck-CrePten*$^{+/-}$ mice (C57BL6/J background) which both carried the Lck-Cre transgene (Hennet et al., 1995) and were heterozygous for the knockout Pten null mutation (Suzuki et al., 1998). Offspring carrying *Lck-Cre* and the floxed *Pten* mutation (*Lck-CrePten*$^{flox/-}$), *Lck-Cre* and *Pten*$^{flox/+}$ (*Lck-CrePten*$^{flox/+}$), and *Lck-Cre* and the wild-type *Pten* gene (*Lck-CrePten*$^{+/+}$) were used for analysis as homozygous mutant, heterozygous mutant, and wild-type mice, respectively. *Lck-CrePten*$^{flox/-}$ mice were chosen rather than *Lck-CrePten*$^{flox/flox}$ animals to maximize the efficiency of gene targeting. *Lck-CrePten*$^{flox/-}$ mice suffering from lymphomas could be distinguished by the presence of abnormally large cells, an overabundance of CD4$^+$ cells, and a marked reduction in B cells, as determined by flow cytometry. These animals were excluded from the analyses.

For thymic selection assays, HY-TCR transgenic *Lck-CrePten*$^{flox/-}$ mice were generated. *Lck-CrePten*$^{flox/+}$ mice (H-2^b) were crossed to *HYPten*$^{+/-}$ mice (H-2^b) heterozygous for the Pten null mutation and carrying the TCR (Vα3Vβ8.2) transgene reactive with the male-specific antigen HY (Teh et al., 1988). Thymocyte and spleen populations in negatively selecting (male) and positively selecting (female) mice were analyzed.

PCR Analysis of Pten Genotypes

Genomic DNA from mouse tails was isolated and amplified by PCR, following a published protocol (Suzuki et al., 1998). Sense primer (5′-GTCACCAGGATGCTTCTGAC-3′) and antisense primer (5′-GAA ACGGCCTTAACGACGTAG-3′) were used to detect the *Ptenflox* allele, sense primer (5′-CCTTGCTCCTGCCGAGAAAGT-3′) and antisense primer (5′-AAAGCACGAGGAAGCGGTCAG-3′) were used to detect the *neo* allele, and sense primer (5′-CCTTGGTGGAGGAGGG TGGAAT-3′) and antisense primer (5′-CCGTCAGTACGTGAGA TATC-3′) were used to detect the *Lck-Cre* transgene. Amplified fragments of 512 bp, 413 bp, and about 900 bp, respectively, were obtained.

Genomic Southern Blot, Western Blots, and Akt Kinase Assay

Genomic Southern blots were performed as described (Suzuki et al., 1998). The probe used is shown in Figure 1A. For protein analyses, thymocytes or peripheral T cells (2×10^7) purified by Thy1.2 magnetic beads (Macs; Miltenyi Biotec Gmbh) were stimulated with immobilized anti-CD3ϵ (10 μg/ml) and anti-CD28 (10 μg/ml) mAbs and/or IL-2 (100 u/ml). Western blots using 50 μg of lysate protein were performed as described (Suzuki et al., 1998). Antibodies directed against the N-terminal end of Pten and anti-IκBα, anti-c-myc (c-8) were from Santa Cruz; anti-phospho-PKB/Akt (S473, Thr308), anti-phospho-Bad (Ser112, 136), anti-phospho-p38 MAPK (Thr180/Tyr182), and anti-phospho-p44/42 MAPK (T202/Y204) were from New England Biolabs; and anti-Bcl-X_L and anti-P27^{kip1} were from Transduction Laboratories; anti-Bcl-2 was from Upstate Biotechnology. The PKB/Akt kinase activity assay was performed as described (Okano et al., 2000).

Serum Immunoglobulin Determinations and Anti-ssDNA Antibodies

Concentrations of serum Ig isotypes were determined by ELISA as described (Kaisho et al., 1997). The measurement of serum anti-ssDNA IgG antibodies was performed using ELISA as described (Satoh et al., 1995).

Flow Cytometric Analysis

The following monoclonal antibodies were used: anti-CD4 (FITC- or PE-conjugated), anti-CD8-PE, anti-Thy1.2-FITC, anti-B220-PE, anti-Vβ8.1/8.2-FITC, anti-Vβ6-FITC, and anti-CD69-PE (all from PharMingen). Stained cells were analyzed with a FACSCalibur (Becton-Dickinson).

T Cell Proliferation, MLR, and Cytokine Production

T cells were purified from MLN using Thy1.2 magnetic beads (Macs; Miltenyi Biotec Gmbh) according to the manufacturer's instructions. Purified T cells (1×10^5) were placed into round-bottomed 96-well plates in RPMI 1640 medium containing 10% FCS. Optimal concentrations (determined in pilot assays) of soluble anti-CD3ε (3 μg/ml), anti-CD28 (10 μg/ml), IL-2 (100 U/ml), Concanavalin A (ConA; 5 μg/ml), or PMA (12.5 ng/ml) plus calcium ionophore (250 ng/ml) were added. T cells were harvested on day 2, after a 12 hr pulse with 1 μCi [^{3}H]thymidine (Amersham) per well. For MLR, lymph node T cells (5×10^5) from 6- to 8-week-old *Pten*$^{flox/-}$ and *Pten*$^{+/+}$ mice were incubated with 5×10^5 γ irradiated (20 Gy) spleen cells from syngeneic (C57BL6/J) or allogeneic (DBA1) mice. Cells were harvested on day 2, and thymidine uptake was assessed as described above. Supernatants of parallel cultures were harvested 30 hr after stimulation and assayed in triplicate for the production of IL-2, IFNγ, IL-4, IL-6, and IL-10 by ELISA according to the manufacturer's (Genzyme) instructions.

In Vivo Injection of SEB

Staphylococcal enterotoxin B (Toxin Technology; 100 μg) was injected intraperitoneally into 6- to 7-week-old mice on day 0. Peripheral blood taken from the tail vein was analyzed by flow cytometry on days 0, 2, 7, 11, and 14. Cells were stained with anti-Vβ8.1/8.2-FITC and anti-CD4-PE, or anti-Vβ6-FITC and anti-CD4-PE.

Thymocyte Apoptosis

Thymocytes (1×10^6) were plated in 24-well plates and treated with various apoptotic stimuli as indicated in Figure 5C. Either 1 or 2 days after treatment, cell viability was determined by staining with either 7-amino-actinomycin D (7-AAD; Sigma) or AnnexinV-PI (R&D Systems) as previously described (Stambolic et al., 1998).

Activation-Induced Cell Death

Purified splenic T cells (4×10^6) were activated for 48 hr at 37°C in 24-well plates in 2 ml RPMI 1640 medium containing 10% FCS, soluble anti-CD3ε (clone 145-2C11; 3 μg/ml), and exogenous murine rIL-2 (R&D; 25 U/ml). Activated T cells were harvested using Lympholyte-M, washed, and 0.5×10^6/ml were replated in 96-well plates with rIL-2, followed by the addition of apoptotic stimuli or withdrawal of rIL-2 and/or serum as shown in Figure 5D. It should be noted that exogenous IL-2 was added to all activated cultures receiving death stimuli (except for those in which IL-2 or serum was withdrawn) to exclude any potential effect of IL-2 withdrawal in these assays. Cell viability was determined 1–3 days poststimulation as described above.

Acknowledgments

We would like to thank Tetsuo Noda (Tohoku University), Shin Yonehara (Kyoto University), Toshifumi Matsuyama (Nagasaki University), Hiroaki Takimoto (Kitazato University), Harumi Suzuki, Satoshi Matsuda (Keio University), Vuk Stambolic, Annick Itie, Wilson Khoo (Amgen Institute), and Nana Iwami (Osaka University) for technical assistance and helpful discussions; Mary Saunders for scientific editing; and Miki Sato Suzuki for her valuable assistance. This work was partially supported by grants from the Ministry of Education, Science, Sports, and Culture, Japan, and from the Future Program of Japanese Society for Promotion of Sciences (JSPS-RFTF98L01101), the National Cancer Institute of Canada (NCIC), and the Canadian Breast Cancer Research Institute (CBCRI).

Received August 18, 2000; revised March 13, 2001.

References

Borlado, L.R., Redondo, C., Alvarez, B., Jimenez, C., Criado, L.M., Flores, J., Marcos, M.A., Martinez, A.C., Balomenos, D., and Carrera, A.C. (2000). Increased phosphoinositide 3-kinase activity induces a lymphoproliferative disorder and contributes to tumor generation in vivo. FASEB J. *14*, 895–903.

Briere, F., Servet-Delprat, C., Bridon, J.M., Saint-Remy, J.M., and Banchereau, J. (1994). Human interleukin 10 induces naive surface immunoglobulin D+ (sIgD+) B cells to secrete IgG1 and IgG3. J. Exp. Med. *179*, 757–762.

Datta, S.R., Dudek, H., Tao, X., Masters, S., Fu, H., Gotoh, Y., and Greenberg, M.E. (1997). Akt phosphorylation of BAD couples survival signals to the cell-intrinsic death machinery. Cell *91*, 231–241.

del Peso, L., Gonzalez-Garcia, M., Page, C., Herrera, R., and Nunez, G. (1997). Interleukin-3 induces phosphorylation of BAD through the protein kinase AKT. Science *278*, 687–689.

Di Cristofano, A., Pesce, B., Cordon-Cardo, C., and Pandolfi, P.P. (1998). Pten is essential for embryonic development and tumour suppression. Nat. Genet. *19*, 348–355.

Di Cristofano, A., Kotsi, P., Peng, Y.F., Cordon-Cardo, C., Elkon, K.B., and Pandolfi, P.P. (1999). Impaired Fas response and autoimmunity in Pten+/- mice. Science *285*, 2122–2125.

Esser, C., and Radbruch, A. (1989). Rapid induction of transcription of unrearranged S gamma 1 switch regions in activated murine B cells by interleukin 4. EMBO J. *8*, 483–488.

Fruman, D.A., Snapper, S.B., Yballe, C.M., Davidson, L., Yu, J.Y., Alt, F.W., and Cantley, L.C. (1999). Impaired B cell development and proliferation in absence of phosphoinositide 3-kinase p85alpha. Science *283*, 393–397.

Ghosh, A.K., Grigorieva, I., Steele, R., Hoover, R.G., and Ray, R.B. (1999). PTEN transcriptionally modulates c-myc gene expression in human breast carcinoma cells and is involved in cell growth regulation. Gene *235*, 85–91.

Gu, H., Zou, Y.R., and Rajewsky, K. (1993). Independent control of immunoglobulin switch recombination at individual switch regions evidenced through Cre-loxP-mediated gene targeting. Cell *73*, 1155–1164.

Gu, J., Tamura, M., and Yamada, K.M. (1998). Tumor suppressor PTEN inhibits integrin- and growth factor-mediated mitogen-activated protein (MAP) kinase signaling pathways. J. Cell Biol. *143*, 1375–1383.

Haas-Kogan, D., Shalev, N., Wong, M., Mills, G., Yount, G., and Stokoe, D. (1998). Protein kinase B (PKB/Akt) activity is elevated in glioblastoma cells due to mutation of the tumor suppressor PTEN/MMAC. Curr. Biol. *8*, 1195–1198.

Hennet, T., Hagen, F.K., Tabak, L.A., and Marth, J.D. (1995). T-cell-specific deletion of a polypeptide N-acetylgalactosaminyl-transferse gene by site-directed recombination. Proc. Natl. Acad. Sci. USA *92*, 12070–12074.

Jones, R.G., Parsons, M., Bonnard, M., Chan, V.S., Yeh, W.C., Woodgett, J.R., and Ohashi, P.S. (2000). Protein kinase B regulates T lymphocyte survival, nuclear factor kappaB activation, and bcl-X(L) levels in vivo. J. Exp. Med. *191*, 1721–1734.

Kaisho, T., Schwenk, F., and Rajewsky, K. (1997). The roles of gamma 1 heavy chain membrane expression and cytoplasmic tail in IgG1 responses. Science *276*, 412–415.

Kappler, J.W., Roehm, N., and Marrack, P. (1987). T cell tolerance by clonal elimination in the thymus. Cell *49*, 273–280.

Kawabe, Y., and Ochi, A. (1991). Programmed cell death and extrathymic reduction of Vbeta8+ CD4+ T cells in mice tolerant to Staphylococcus aureus enterotoxin B. Nature *349*, 245–248.

Kaye, J., Hsu, M.L., Sauron, M.E., Jameson, S.C., Gascoigne, N.R., and Hedrick, S.M. (1989). Selective development of CD4+ T cells

in transgenic mice expressing a class II MHC-restricted antigen receptor. Nature *341*, 746–749.

Kim, C., Siminovitch, K.A., and Ochi, A. (1991). Reduction of lupus nephritis in MRL/lpr mice by a bacterial superantigen treatment. J. Exp. Med. *174*, 1431–1437.

Kinzler, K.W., and Vogelstein, B. (1998). Landscaping the cancer terrain. Science *280*, 1036–1037.

Kisielow, P., Bluthmann, H., Staerz, U.D., Steinmetz, M., and von Boehmer, H. (1988). Tolerance in T-cell-receptor transgenic mice involves deletion of nonmature CD4+8+ thymocytes. Nature *333*, 742–746.

Li, J., Yen, C., Liaw, D., Podsypanina, K., Bose, S., Wang, S.I., Puc, J., Miliaresis, C., Rodgers, L., McCombie, R., et al. (1997). PTEN, a putative protein tyrosine phosphatase gene mutated in human brain, breast, and prostate cancer. Science *275*, 1943–1947.

Li, D.M., and Sun, H. (1998). PTEN/MMAC1/TEP1 suppresses the tumorigenicity and induces G1 cell cycle arrest in human glioblastoma cells. Proc. Natl. Acad. Sci. USA *95*, 15406–15411.

Liao, X.C., and Littman, D.R. (1995). Altered T cell receptor signaling and disrupted T cell development in mice lacking Itk. Immunity *3*, 757–769.

Liaw, D., Marsh, D.J., Li, J., Dahia, P.L., Wang, S.I., Zheng, Z., Bose, S., Call, K.M., Tsou, H.C., Peacocke, M., et al. (1997). Germline mutations of the PTEN gene in Cowden disease, an inherited breast and thyroid cancer syndrome. Nat. Genet. *16*, 64–67.

Maehama, T., and Dixon, J.E. (1998). The tumor suppressor, PTEN/MMAC1, dephosphorylates the lipid second messenger, phosphatidylinositol 3,4,5-trisphosphate. J. Biol. Chem. *273*, 13375–13378.

Marsh, D.J., Dahia, P.L., Zheng, Z., Liaw, D., Parsons, R., Gorlin, R.J., and Eng, C. (1997). Germline mutations in PTEN are present in Bannayan-Zonana syndrome. Nat. Genet. *16*, 333–334.

Marsh, D.J., Kum, J.B., Lunetta, K.L., Bennett, M.J., Gorlin, R.J., Ahmed, S.F., Bodurtha, J., Crowe, C., Curtis, M.A., Dasouki, M., et al. (1999). PTEN mutation spectrum and genotype-phenotype correlations in Bannayan-Riley-Ruvalcaba syndrome suggest a single entity with Cowden syndrome. Hum. Mol. Genet. *8*, 1461–1472.

Myers, M.P., Pass, I., Batty, I.H., Van der Kaay, J., Stolarov, J.P., Hemmings, B.A., Wigler, M.H., Downes, C.P., and Tonks, N.K. (1998). The lipid phosphatase activity of PTEN is critical for its tumor supressor function. Proc. Natl. Acad. Sci. USA *95*, 13513–13518.

Okano, J., Gaslightwala, I., Birnbaum, M.J., Rustgi, A.K., and Nakagawa, H. (2000). Akt/protein kinase B isoforms are differentially regulated by epidermal growth factor stimulation. J. Biol. Chem. *275*, 30934–30942.

Ozes, O.N., Mayo, L.D., Gustin, J.A., Pfeffer, S.R., Pfeffer, L.M., and Donner, D.B. (1999). NF-kappaB activation by tumour necrosis factor requires the Akt serine-threonine kinase. Nature *401*, 82–85.

Podsypanina, K., Ellenson, L.H., Nemes, A., Gu, J., Tamura, M., Yamada, K.M., Cordon-Cardo, C., Catoretti, G., Fisher, P.E., and Parsons, R. (1999). Mutation of Pten/Mmac1 in mice causes neoplasia in multiple organ systems. Proc. Natl. Acad. Sci. USA *96*, 1563–1568.

Pugazhenthi, S., Nesterova, A., Sable, C., Heidenreich, K.A., Boxer, L.M., Heasley, L.E., and Reusch, J.E. (2000). Akt/protein kinase B up-regulates Bcl-2 expression through camp-response element-binding protein. J. Biol. Chem. *275*, 10761–10766.

Romashkova, J.A., and Makarov, S.S. (1999). NF-kappaB is a target of AKT in anti-apoptotic PDGF signalling. Nature *401*, 86–90.

Sasaki, T., Irie-Sasaki, J., Jones, R.G., Oliveira-dos-Santos, A.J., Stanford, W.L., Bolon, B., Wakeham, A., Itie, A., Bouchard, D., Kozieradzki, I., et al. (2000). Function of PI3Kgamma in thymocyte development, T cell activation, and neutrophil migration. Science *287*, 1040–1046.

Satoh, M., Kumar, A., Kanwar, Y.S., and Reeves, W.H. (1995). Anti-nuclear antibody production and immune-complex glomerulonephritis in BALB/c mice treated with pristane. Proc. Natl. Acad. Sci. USA *92*, 10934–10938.

Sebzda, E., Mariathasan, S., Ohteki, T., Jones, R., Bachmann, M.F., and Ohashi, P.S. (1999). Selection of the T cell repertoire. Annu. Rev. Immunol. *17*, 829–874.

Shan, X., Czar, M.J., Bunnell, S.C., Liu, P., Liu, Y., Schwartzberg, P.L., and Wange, R.L. (2000). Deficiency of Pten in Jurkat T cells causes constitutive localization of Itk to the plasma membrane and hyperresponsiveness to CD3 stimulation. Mol. Cell. Biol. *20*, 6945–6957.

Sharp, L.L., and Hedrick, S.M. (1999). Commitment to the CD4 lineage mediated by extracellular signal-related kinase mitogen-activated protein kinase and lck-signaling. J. Immunol. *163*, 6598–6605.

Stambolic, V., Suzuki, A., de la Pompa, J.L., Brothers, G.M., Mirtsos, C., Sasaki, T., Ruland, J., Penninger, J.M., Siderovski, D.P., and Mak, T.W. (1998). Negative regulation of PKB/Akt-dependent cell survival by the tumor suppressor PTEN. Cell *95*, 29–39.

Staszak, C., and Harbeck, R.J. (1985). Mononuclear-cell pulmonary vasculitis in NZB/W mice. I. Histopathologic evaluation of spontaneously occurring pulmonary infiltrates. Am. J. Pathol. *120*, 99–105.

Sugawara, T., Moriguchi, T., Nishida, E., and Takahama, Y. (1998). Differential roles of ERK and p38 MAP kinase pathways in positive and negative selection of T lymphocytes. Immunity *9*, 565–574.

Suzuki, A., de la Pompa, J.L., Stambolic, V., Elia, A.J., Sasaki, T., del Barco Barrantes, I., Ho, A., Wakeham, A., Itie, A., Khoo, W., et al. (1998). High cancer susceptibility and embryonic lethality associated with mutation of the PTEN tumor suppressor gene in mice. Curr. Biol. *8*, 1169–1178.

Suzuki, H., Terauchi, Y., Fujiwara, M., Aizawa, S., Yazaki, Y., Kadowaki, T., and Koyasu, S. (1999). Xid-like immunodeficiency in mice with disruption of the p85alpha subunit of phosphoinositide 3-kinase. Science *283*, 390–392.

Teh, H.S., Kisielow, P., Scott, B., Kishi, H., Uematsu, Y., Bluthmann, H., and von Boehmer, H. (1988). Thymic major histocompatibility complex antigens and the alpha beta T-cell receptor determine the CD4/CD8 phenotype of T cells. Nature *335*, 229–233.

Toker, A., and Cantley, L.C. (1997). Signalling through the lipid products of phosphoinositide-3-OH kinase. Nature *387*, 673–676.

Volkers, N. (1999). Do autoimmune diseases raise the risk of cancer? J. Natl. Cancer. Inst. *91*, 1992–1993.

Webb, S., Morris, C., and Sprent, J. (1990). Extrathymic tolerance of mature cells: clonal elimination as a consequence of Immunity. Cell *63*, 1249–1256.

Yamamoto, K., Doyle, C., Miele, L., and Germain, R.N. (2000). The duration of antigen receptor signalling determines $CD4^+$ versus $CD8^+$ T-cell lineage fate. Nature *404*, 506–510.